Supplementary Information for

Critical Interplay of Defect Engineering and Plasmonics in Hybrid Nanostructures for Ultrasensitive Photo-Enhanced Raman Spectroscopy

Arti Sharma[1, ‡], Shubhadip Atta[2, ‡], Shubham Sharma[3], Prashant Mishra[3], Soutik Betal[2], Soumik Siddhanta[1*]*

1. Department of Chemistry, Indian Institute of Technology Delhi, Hauz Khas, New Delhi, 110016, India

2. Department of Electrical Engineering, Indian Institute of Technology Delhi, Hauz Khas, New Delhi, 110016, India

3. Department of Biochemical Engineering and Biotechnology, Indian Institute of Technology Delhi, Hauz Khas, New Delhi, 110016, India

‡Arti and Shubhadip Shared first authorship (both authors contributed equally to the manuscript)

*Corresponding authors: soumik@iitd.ac.in, soutik@ee.iitd.ac.in

Table of Contents

Figure S8. Valence band XPS spectra of TiO_2_500, TiO_2_700, and TiO_2_USP samples. The valence band edge was determined by extrapolating the linear portion of the leading edge to the baseline. The extracted VBM values are 2.46 eV for TiO_2_500, 2.33 eV for TiO_2_700, and 2.69 eV for TiO_2_USP, showing a clear shift in electronic states depending on the synthesis and treatment conditions.

Enhancement Factor Calculation

The enhancement factor (EF) for surface-enhanced Raman spectroscopy (SERS) and photoinduced enhanced Raman spectroscopy (PIERS) was calculated using the following expression, as also done elsewhere[1]

$$EF_{SERS}\,(\omega_v) = \frac{I_{SERS}}{I_{Raman}} \times \frac{N_{Bulk}}{N_{surface}}$$

$$EF_{PIERS}\,(\omega_v) = \frac{I_{PIERS}}{I_{Raman}} \times \frac{N_{Bulk}}{N_{surface}}$$

Where N_{bulk} and $N_{surface}$ are given as:

N_{bulk} can be given as $\frac{A\ laser\ X\ h\ X\ \rho}{M} * N_A$

$N_{surface}$ can be given as $\frac{C\ X\ V}{A_{substrate}} * N_A * A_{laser}$

A_{laser} is the area of the laser spot (1.445×10^{-7} cm^2),

h is the focal depth of the laser (0.03 cm),

ρ is the density of the analyte (1.26 g cm^{-3}),

M is the molecular weight of the analyte (479.02 g mol^{-1}), and

N_A is Avogadro's number (6.022×10^{23} mol^{-1}).

C is the molar concentration of the analyte (either 10^{-7} or 10^{-5} mol L^{-1}),

V is the volume of the analyte solution used (10 µL or 1×10^{-5} L),

$A_{substrate}$ is the area of the substrate (0.2513 cm^2)

Calculation of Energy levels for Titanium oxide from XPS

The Valence Band Maximum (VBM) was initially determined through a linear extrapolation of the TiO_2 XPS valence band leading edge to the baseline. This method provided binding energy relative to the Fermi level. To convert the valence band edge to the absolute vacuum energy scale, a work function (ϕ) of 5 eV was utilized. This approach enabled the calculation of the absolute valence band maximum energy relative to the vacuum energy. The position of the Conduction Band minimum was then determined by adding the optical band gap to the previously obtained value.

$$E_{Valence\ band\ maxima} = \phi - BE_{Valence\ band\ maxima}$$

Tables

Table S1: Shows the enhancement factor of both SERS and PIERS

Sample	Raman Intensity (a.u.)	SERS Intensity	EF	PIERS Intensity	EF	PIERS/SERS
Sol_500 (10^{-7})	27.4	95	5.43×10^{7}	600	4.34×10^{8}	6.32
Sol_700 (10^{-7})		75	6.88×10^{7}	418.23	3.03×10^{8}	5.58
USP_700 (10^{-7})		25	1.81×10^{7}	35	2.53×10^{7}	1.40
Sol_500 (10^{-5})	177	490	5.49×10^{5}	2450	2.74×10^{6}	5.00
Sol_700 (10^{-5})		580	6.50×10^{5}	1700	1.90×10^{6}	2.93
USP_700 (10^{-5})		900	1.01×10^{6}	100	1.12×10^{5}	0.11

Table S2: Raman peaks corresponding to different phases of TiO_2

Phase (Space Group)	**Raman Shift (cm^{-1})**	**Symmetry Mode**
Anatase	144	E_g
($I4_1/amd$)	397	B_{1g}
	513	A_{1g}
	519	B_{1g}
	639	E_g
Rutile	147	B_{1g}
($P4_2/mnm$)	240	Multi-phonon
	438	E_g
	612	A_{1g}
	810	B_{2g}

Table S3: Tentative Raman vibrational mode assignment of the R6G molecule

Raman shift (cm^{-1})	Tentative Raman vibrational modes of proteins[2, 3, 4]
612	in-plane bending ring vibration (C-C-C)
773	Aromatic C-H out-of-plane bending
1127	Aromatic C-H in-plane bending
1180	C-C stretching coupled with C-H bending
1311	C-N (xanthene ring)
1363	C-C stretching (Aromatic)
1514	C-C stretching (Aromatic)
1656	C-C stretching (Aromatic)

Table S4: XPS fitting results of Titanium 2p spectra

Sample	Full-width half maxima Ti^{4+} $2p_{1/2}$	Full-width half-maxima Ti^{4+} $2p_{3/2}$	Area of Ti^{4+} $2p_{3/2}$	Area of Ti^{4+} $2p_{3/2}$ value	Area Ratio of $2P_{3/2}$: $2P_{1/2}$	Ti^{4+} $2p_{1/2}$ – Ti^{4+} $2p_{3/2}$ Splitting
TiO_2 (Sol-500)	1.65393853737	0.89868691882	17561.016647	8904.90773906	1.97	5.55 eV
TiO_2 (USP-700)	1.68459117722	0.89572283920	25300.1248845	12644.7638581	2.00	5.90 eV
TiO_2 (Sol-700)	1.65486711857	0.89736067199	16564.7253282	8912.8586158	1.85	5.54 eV

Table S5: Surface reduction quantification in TiO_2 samples using Ti 2p XPS peak areas

Sample	Ti^{3+} $2p_{3/2}$ Area	Ti^{4+} $2p_{3/2}$ Area	Ti^{3+} Fraction (%)
TiO_2 (Sol-500)	5554.44	17561.02	24.03%
TiO_2 (Sol-700)	4031.69	16564.73	19.58%
TiO_2 (USP-700)	absent	25,300.12	-

Table S6: Quantitative analysis of oxygen vacancy concentration in TiO_2 samples obtained from O 1s XPS peak deconvolution.

Sample	Lattice O (O^{2-}) Binding Energy (eV)	Area	Oxygen Vacancy (O_v) Binding Energy (eV)	Area	Surface –OH Binding Energy (eV)	Area	Oxygen Defect Fraction (%)
TiO_2 (Sol–gel, 700°C)	529.5	15635.488	530.3	15799.10	531.8	2648.814	46.35
TiO_2 (Sol–gel, 500°C)	529.5	11625.943	530.2	19264.04	532.2	2370.035	57.92
TiO_2 (USP, 700°C)	529.8	33691.154	-	-	531.7	18640.81	-

Figures

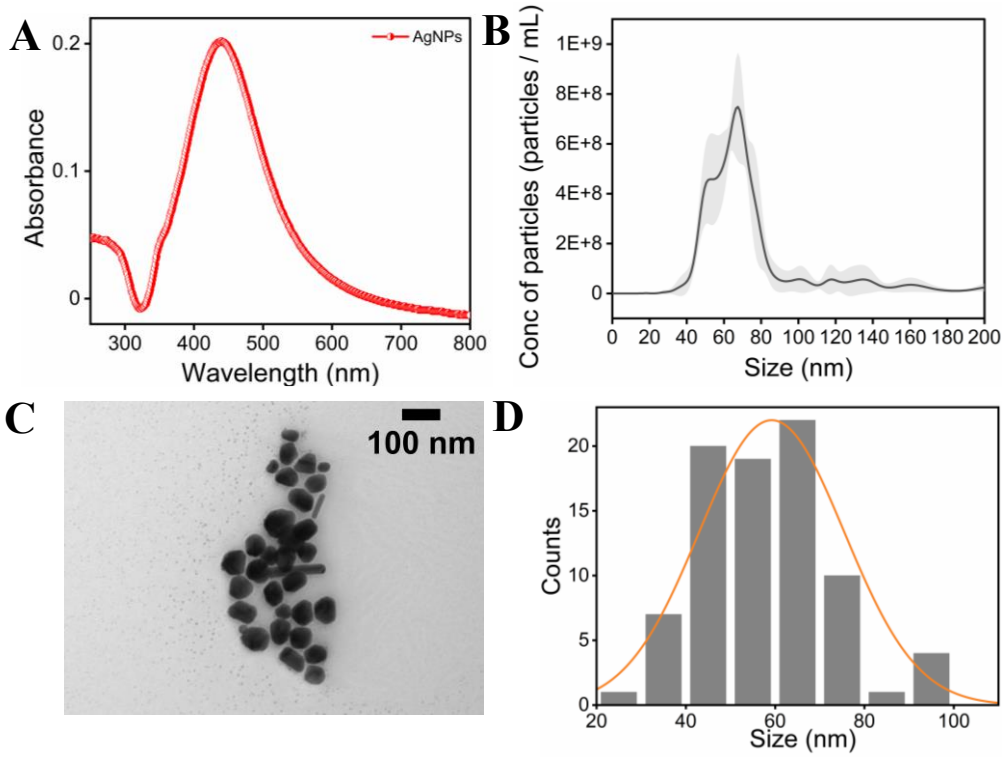

Figure S1. A) Shows the plasmonic peak for AgNPs at 441 nm. B) Shows the average size of AgNPs with the Nanoparticle tracking analyzer. C) Show the TEM image of the AgNPs at a 100 nm scale. D) size distribution analysis of the AgNPs analyzed using the ImageJ software.

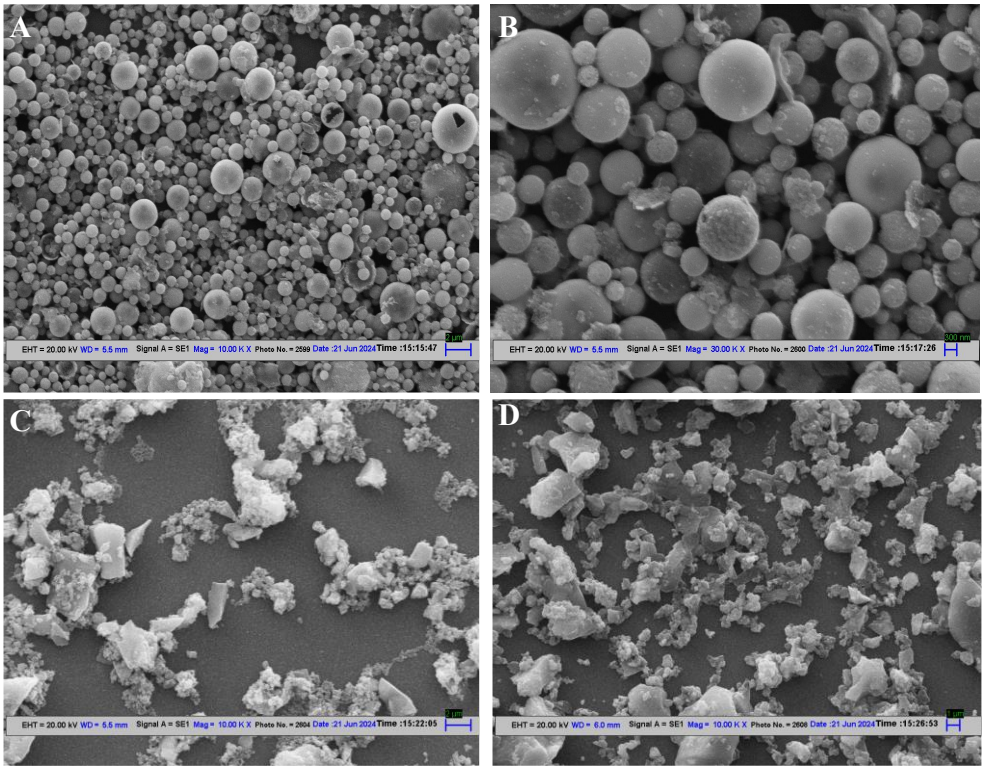

Figure S2. (A, B) Shows the Scanning electron microscope (SEM) images of synthesized TiO_2 (USP_700), (C) TiO_2 (Sol_700), and (D) TiO_2 (Sol_500).

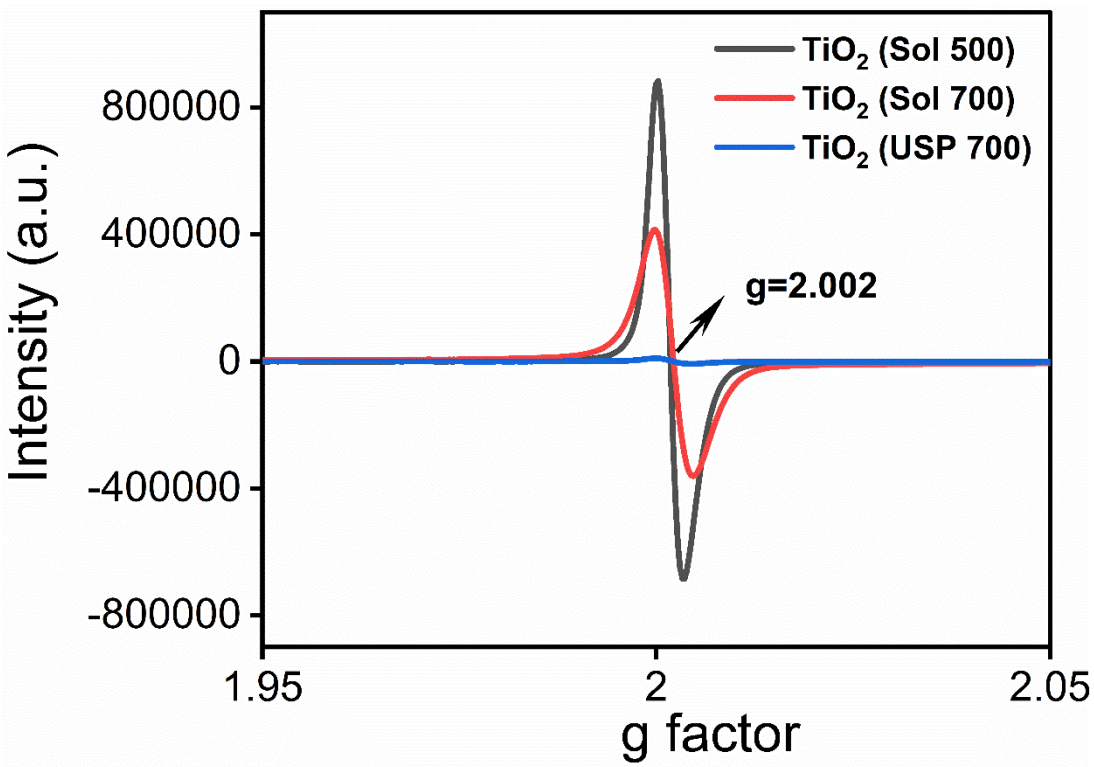

Figure S3. EPR spectra of TiO_2 (Sol-500), TiO_2 (Sol-700), and TiO_2 (USP-700) are shown in black, red, and blue, respectively.

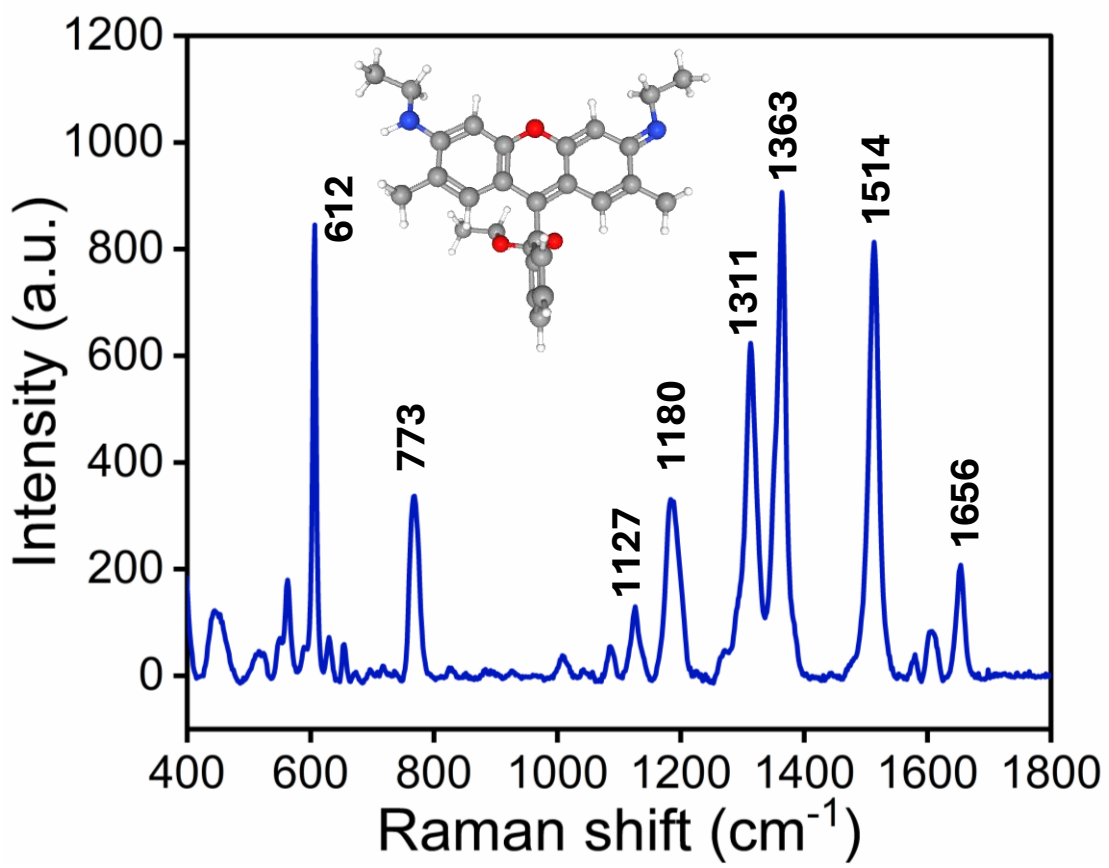

Figure S4. Characteristic Raman fingerprint region of the R6G molecule.

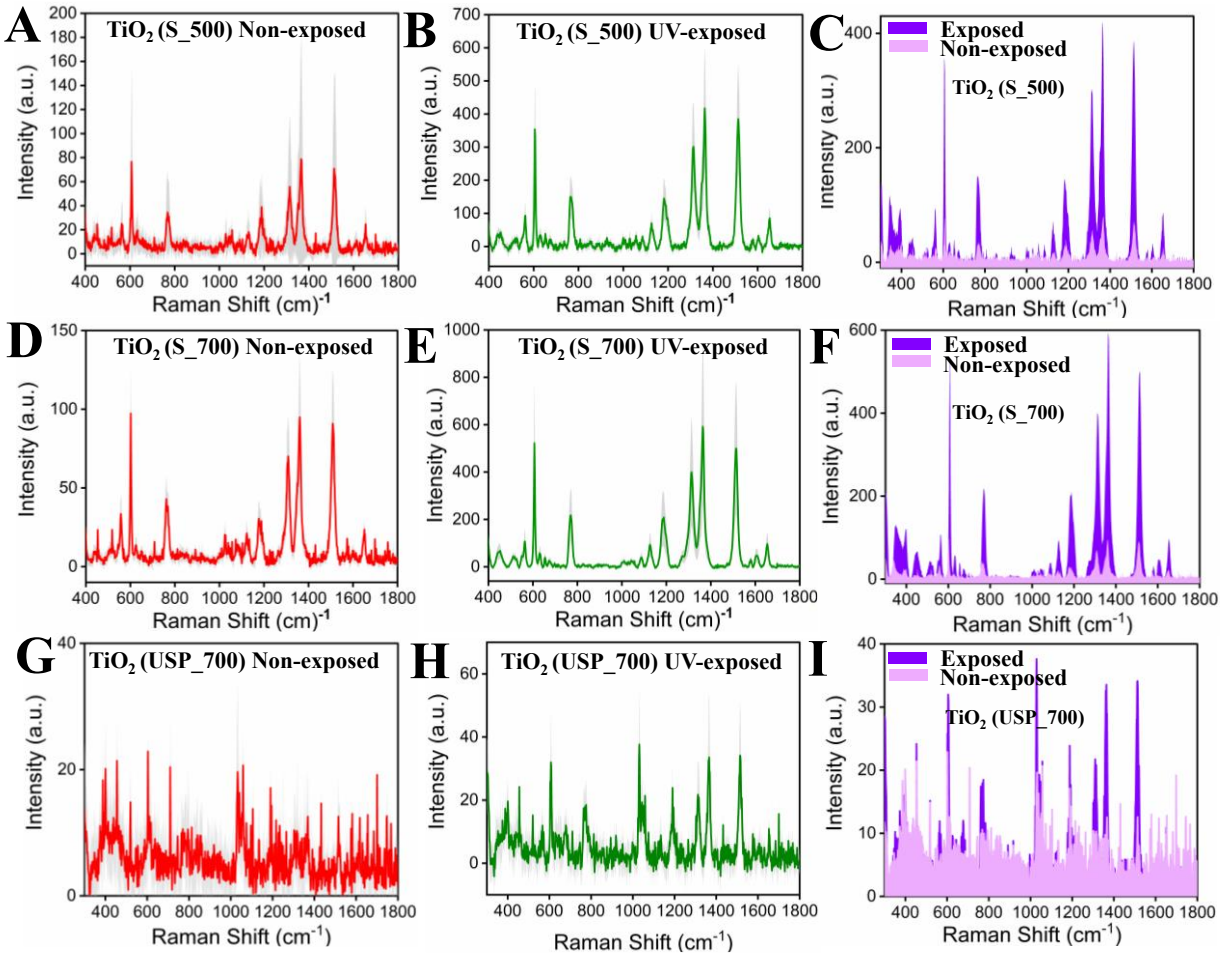

Figure S5. (A, B) Shows the Raman spectrum of the R6G molecule at a concentration of 10^{-7} M for non-UV irradiated and after UV irradiation of the TiO_2 (S_500) sample. (C) Shows the overlaid Raman spectrum of TiO_2 (S_500) to show the intensity difference before and after UV irradiation. (D, E) Shows the Raman spectrum of the R6G molecule at a concentration of 10^{-7} M for non-UV irradiation and after UV irradiation of the TiO_2 (S_700) sample. (F) Shows the overlaid Raman spectrum of TiO_2 (S_700) to show the intensity difference before and after UV irradiation. (G, H) Shows the Raman spectrum of the R6G molecule at a concentration of 10^{-7} M for non-UV irradiated and after UV irradiation of the TiO_2 (USP_700) sample. (I) Shows the overlaid Raman spectrum of TiO_2 (USP_700) to show the intensity difference before and after UV irradiation.

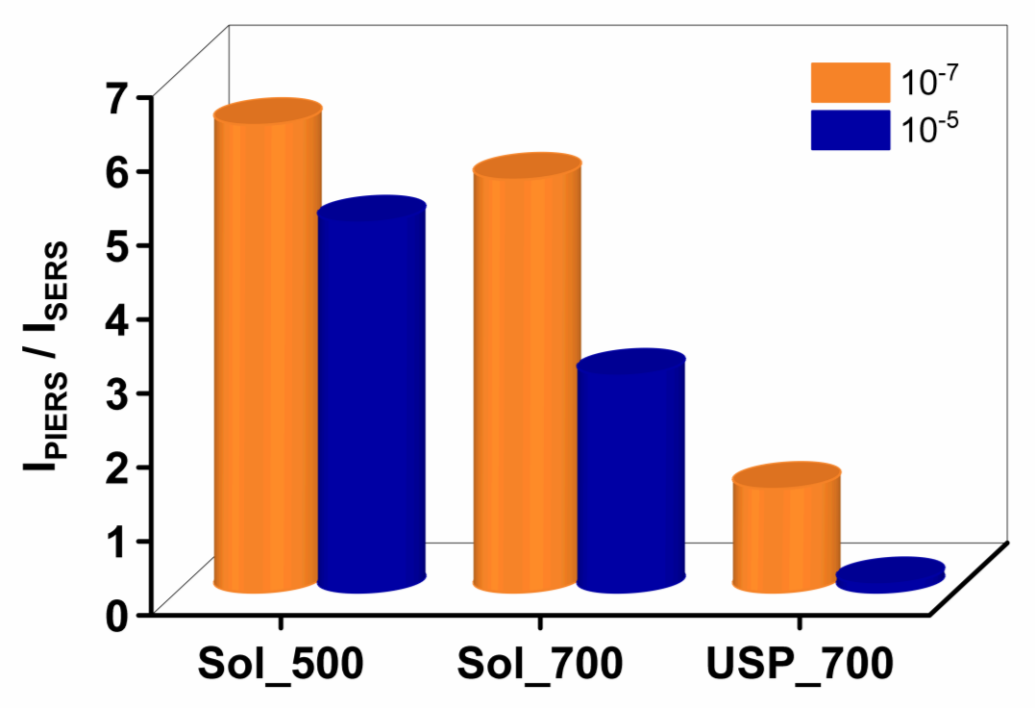

Figure S6. Shows the enhancement factor for TiO_2(S_500), TiO_2 (S_700), and TiO2_(USP_700) based on the calculation done in Table 1.

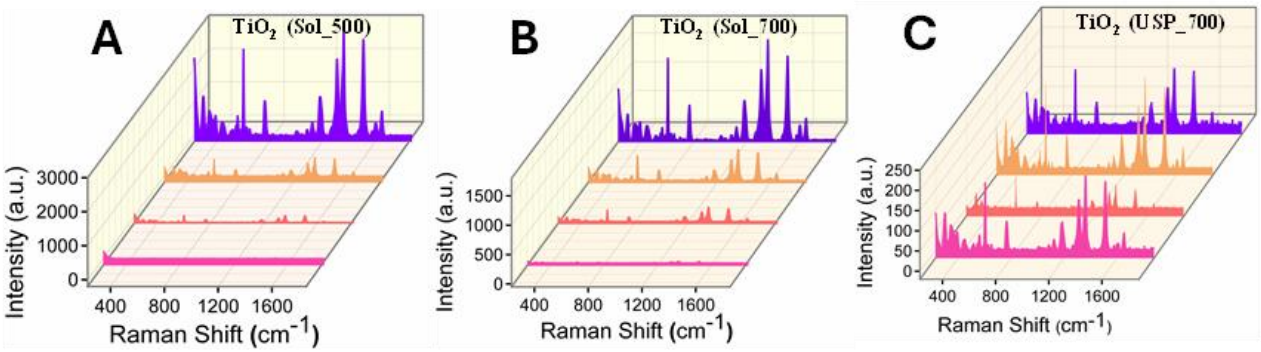

Figure S7. Shows the Raman spectrum for the R6G at 10^{-5} M concentration for differently synthesized TiO_2 samples in the following order: TiO_2-R6G (Pink), TiO_2_R6G_UV irradiated (brick red), TiO_2_AgNPs_R6G (Orange), TiO_2_AgNPs_R6G_UV irradiated (violet).

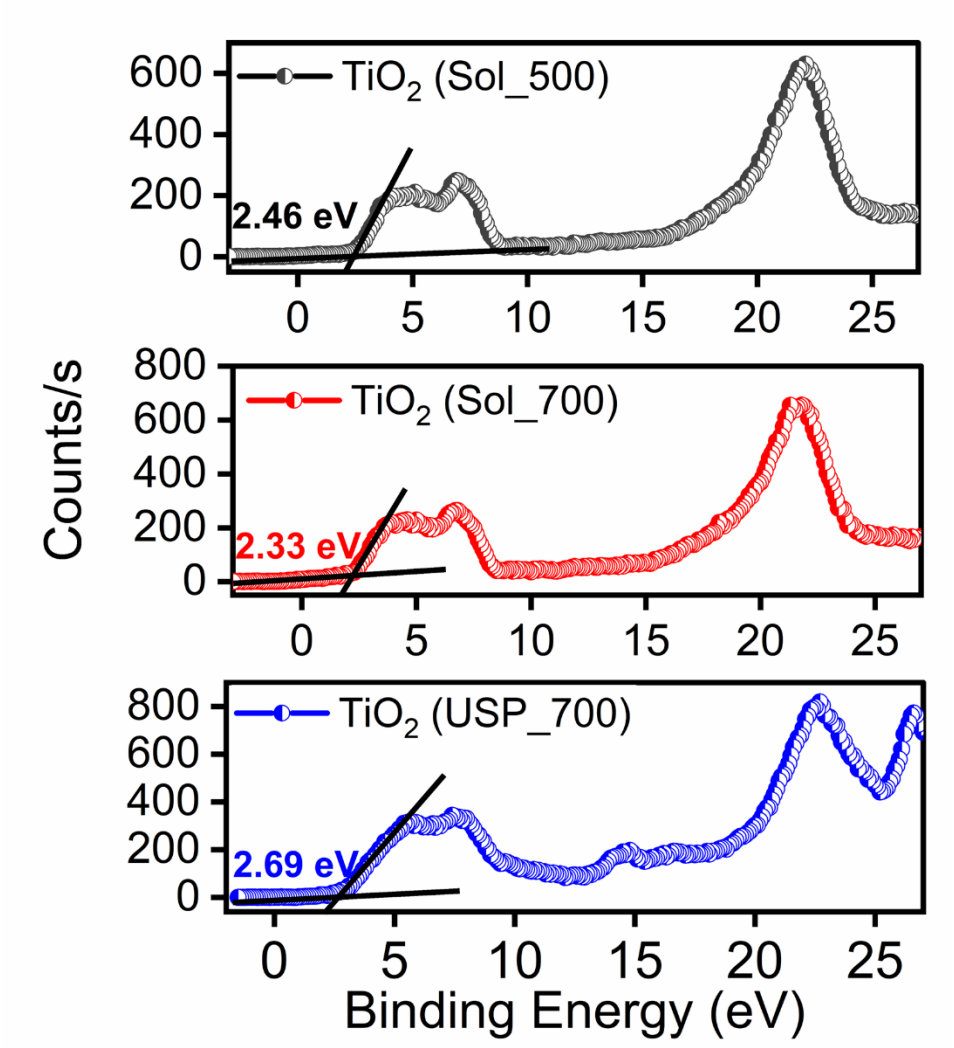

Figure S8. Valence band XPS spectra of TiO_2_500, TiO_2_700, and TiO_2_USP samples. The valence band edge was determined by extrapolating the linear portion of the leading edge to the baseline. The extracted VBM values are 2.46 eV for TiO_2_500, 2.33 eV for TiO_2_700, and 2.69 eV for TiO_2_USP, showing a clear shift in electronic states depending on the synthesis and treatment conditions.

References

1. S. Ben-Jaber, W. J. Peveler, R. Quesada-Cabrera, E. Cortés, C. Sotelo-Vazquez, N. Abdul-Karim, S. A. Maier and I. P. Parkin, Nature communications, 2016, 7, 12189.
2. P. Hildebrandt and M. Stockburger, The Journal of Physical Chemistry, 1984, 88, 5935-5944.
3. D. Huang, J. Cui and X. Chen, Colloids and Surfaces A: Physicochemical and Engineering Aspects, 2014, 456, 100-107.
4. X. N. He, Y. Gao, M. Mahjouri-Samani, P. N. Black, J. Allen, M. Mitchell, W. Xiong, Y. S. Zhou, L. Jiang and Y. F. Lu, Nanotechnology, 2012, 23, 205702.